Supporting Information

Donor-acceptor-donor structured thioxanthone derivatives as visible photoinitiators

Alexandre Mau [a b], Thi Huong Le [c], Céline Dietlin [a b], Thanh-Tuân Bui*[c], Bernadette Graff [a b], Frédéric Dumur [d], Fabrice Goubard [c], and Jacques Lalevee*[a b]

[a] *Université de Haute-Alsace, CNRS, IS2M UMR 7361, F-68100 Mulhouse, France*

[b] *Université de Strasbourg, France*

[c] *CY Cergy Paris Université, LPPI, F-95000 Cergy, France.*

[d] *Aix Marseille Univ, CNRS, ICR, UMR 7273, F-13397 Marseille, France*

* Corresponding author: tbui@cyu.fr (T.-T. B.); jacques.lalevee@uha.fr (J. L.)

Synthesis protocols

General method for the synthesis of **TX-2DPA** and **TX-2PTz** (Buchwald-Hartwig coupling reaction):

In the dried Schlenk flask, 2,7-dibromo-9H-thioxanthen-9-one[1] and diarylamine were dissolved in distillated toluene under argon atmosphere. Then, palladium catalyst $PdCl_2(PPh_3)_4$ (0.2 eq) and sodium-*tert*-butoxide (10.0 eq) were added to the mixture reaction. The reaction mixture was stirred under argon atmosphere while the temperature was slowly raised to 110^{o}C and kept in 24h. Reaction mixture was then cooled to room temperature. The solution was filtered through short silica path to remove catalysts. All organic phases were combined and evaporated to get the crude product which was further purified by column chromatography.

2,7-bis(bis(4-methoxyphenyl)amino)-9H-thioxanthen-9-one (**TX-2DPA**): A mixture of 2,7-dibromo-9H-thioxanthen-9-one (200mg, 1eq) and 4.4′-dimethoxydiphenylamine (386mg, 3eq), $PdCl_2(PPh_3)_4$ (28mg, 0.1eq) and NaO*t*Bu (520mg, 10eq) were reacted as mentioned in general method. The obtained crude product was purified by column chromatography using petroleum ethers: ethyl acetate (9:1 v/v) to obtain a red solid (189mg, 50% yield). ^{1}H NMR (250 MHz, DMSO-d6) δ 7.66 (d, *J* =2.5 Hz, 1H), 7.61 (m, 1H), 7.19 (d, *J* = 10 Hz, 1H), 7.1 (d, *J* = 7.5 Hz, 4H), 6.95 (d, *J* =7.5 Hz, 4H,), 3.75 (s, 6H). ^{13}C NMR (62.5 MHz, DMSO-d_6) δ 184.4, 156.8, 147.8, 139.7, 129.0, 127.6, 115.6, 55.7.

2,7-di(10H-phenothiazin-10-yl)-9H-thioxanthen-9-one (**TX-2PTz**): A mixture of 2,7-dibromo-9H-thioxanthen-9-one (200mg, 0.54 mmol, 1eq) and phenothiazine (325mg, 1.63 mmol, 3eq), $PdCl_2(PPh_3)_4$ (38mg, 0.054 mmol, 0.1eq) and NaOtBu (520mg, 5.4 mmol, 10eq) were mixed in 15ml of toluene as mentioned in general method. The obtained crude product was purified by column chromatography using petroleum ethers: ethyl acetate (9:1 v/v) to obtain a yellow solid (300mg, 90% yield). ^{1}H NMR (250 MHz, $CDCl_3$) δ 8.66 (d, *J* = 2.5 Hz, 1H), 7.81 (d, *J* = 10 Hz, 1H), 7.67 (dd, J_1 = 2.5Hz, J_2 = 7.5Hz, 1H), 7.14 (dd, J_1 = 2.5Hz, J_2 = 7.5Hz, 2H), 6.93 (m, 4H), 6.46 (dd, J_1 = 2.5Hz, J_2 = 7.5Hz, 2H). ^{13}C NMR (62.5 MHz, $CDCl_3$) δ 178.8, 143.5, 140.6, 135.4, 133.2, 130.5, 129.8, 128.6, 127.3, 127.0, 123.5, 123.1, 118.0. HRMS (ESI-MS): calculated for $C_{37}H_{22}N_2OS_3$ $[M+H]^+$: 607.0894; found: 607.0967.

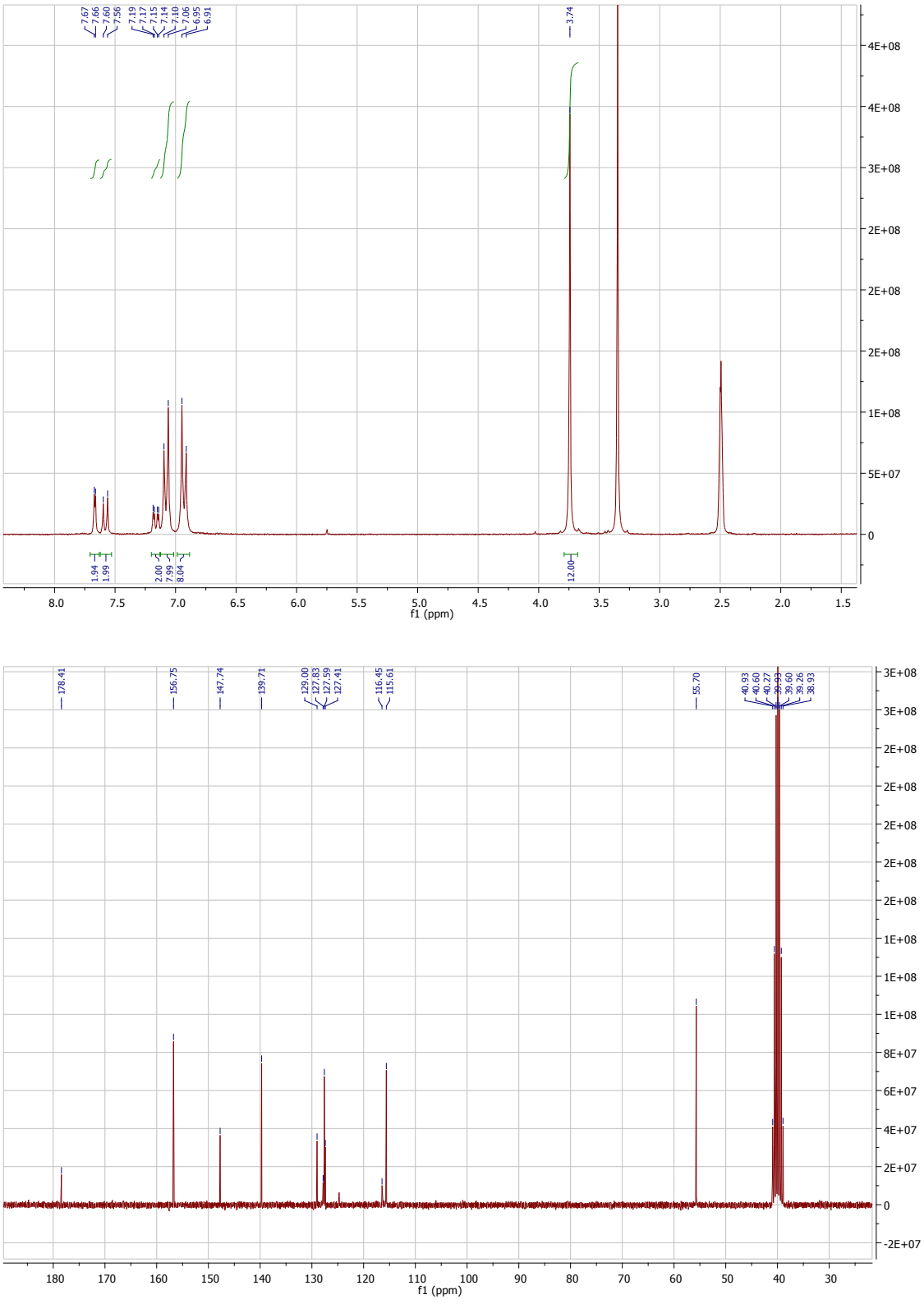

Figure S1. ^{1}H NMR (above) and ^{13}C NMR (below) spectra for **TX-2DPA** in DMSO-d_6.

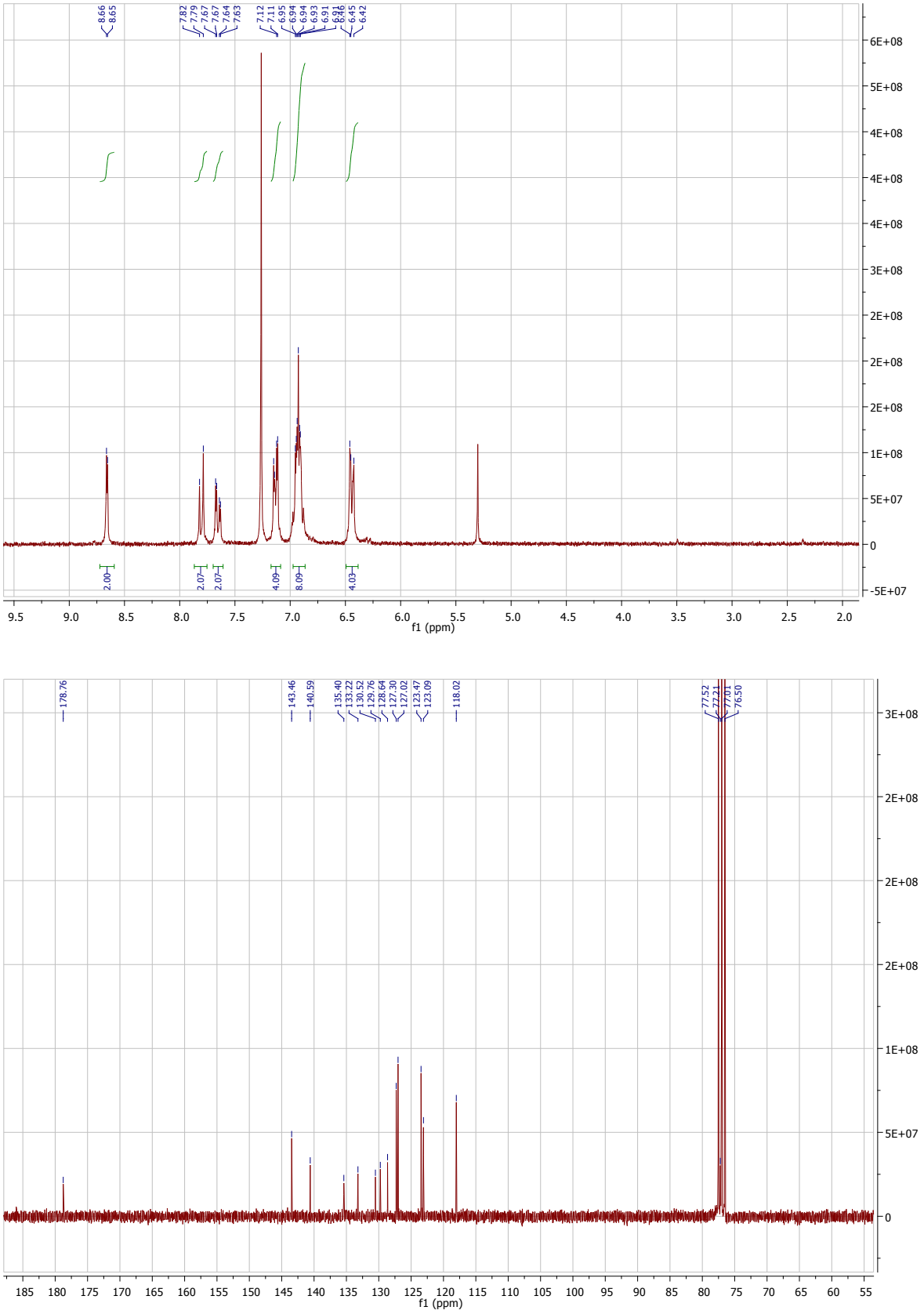

Figure S2. ^{1}H NMR (above) and ^{13}C NMR (below) spectra for **TX-2PTz** in $CDCl_3$.

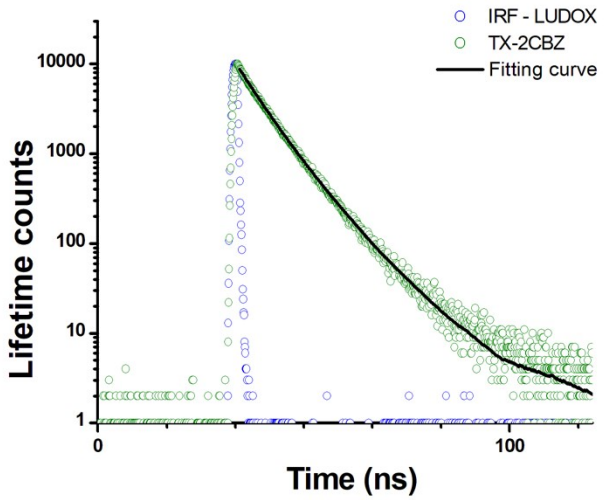

Figure S3: Time-correlated single-photon counting of TX-2CBZ in dichloromethane, λ_{ex}= 367 nm, λ_{em} = 502 nm and [TX-2CBZ] = 1.4×10^{-5} mol.L^{-1}, two exponential curve fitting.

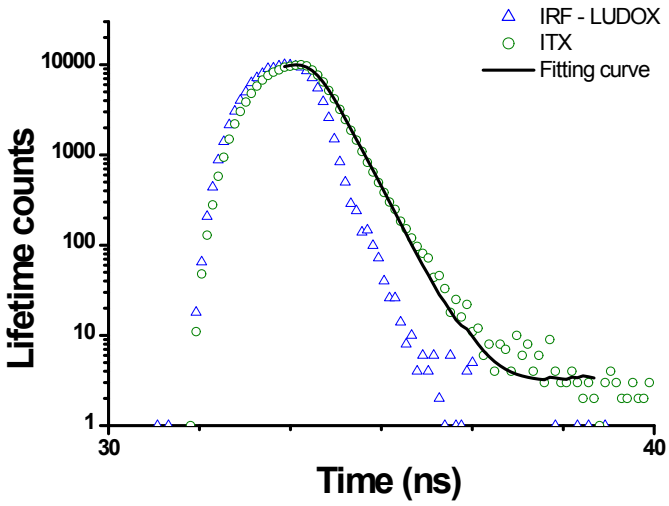

Figure S4: Time-correlated single photon counting of ITX in dichloromethane, λ_{ex}=367nm, λ_{em}=502 nm and [ITX]=1.4 x10^{-5} mol.L^{-1}

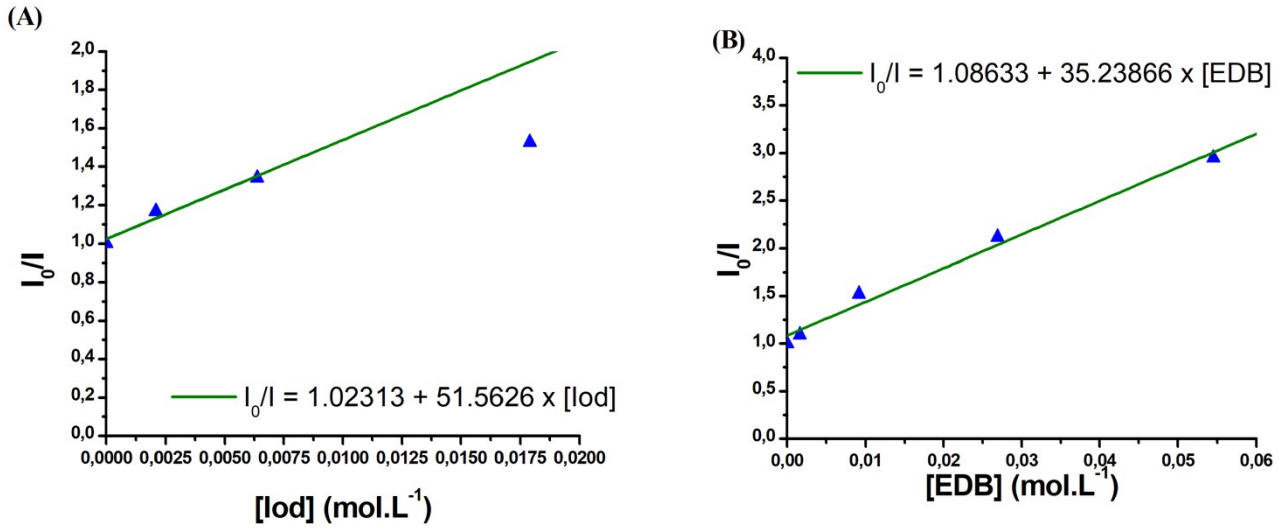

Figure S5: Stern-Volmer quenching plots of singlet excited state TX-2CBZ obtained by steady state fluorescence, λ_{ex}=400 nm, λ_{em}=502 nm (A) quencher = Iod, [TX-2CBZ] = 1.7 x 10^{-5} mol.L^{-1}, the experimental data point for [Iod] = 1.79x10^{-2} mol.L^{-1} is excluded from the linear regression due to the non-neglectable absorption at 400 nm of Iod which could explains the deviation at this higher concentration ; (B) quencher = EDB, [TX-2CBZ]= 3.3 x 10^{-5} mol.L^{-1}

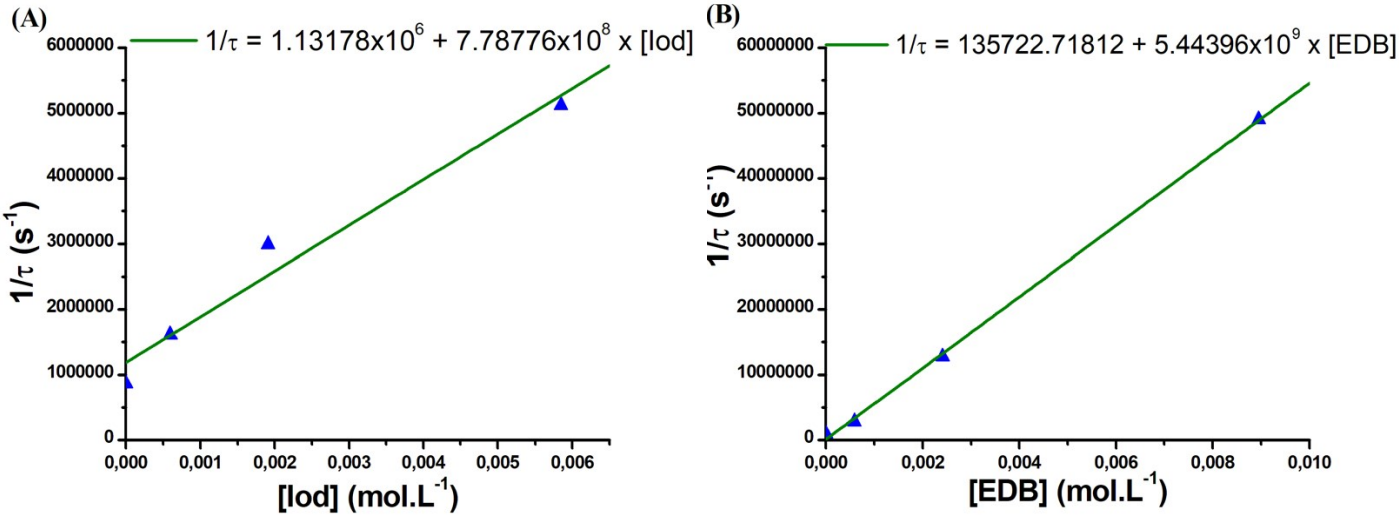

Figure S6: Stern-Volmer quenching plots of triplet excited state TX-2CBZ obtained by laser flash photolysis, record at 655 nm, excitation at 355 nm (A) quencher = Iod, [TX-2CBZ] = 5.8 x 10^{-5} mol.L^{-1}; (B) quencher = EDB, [TX-2CBZ]= 5.3 x 10^{-5} mol.L^{-1}

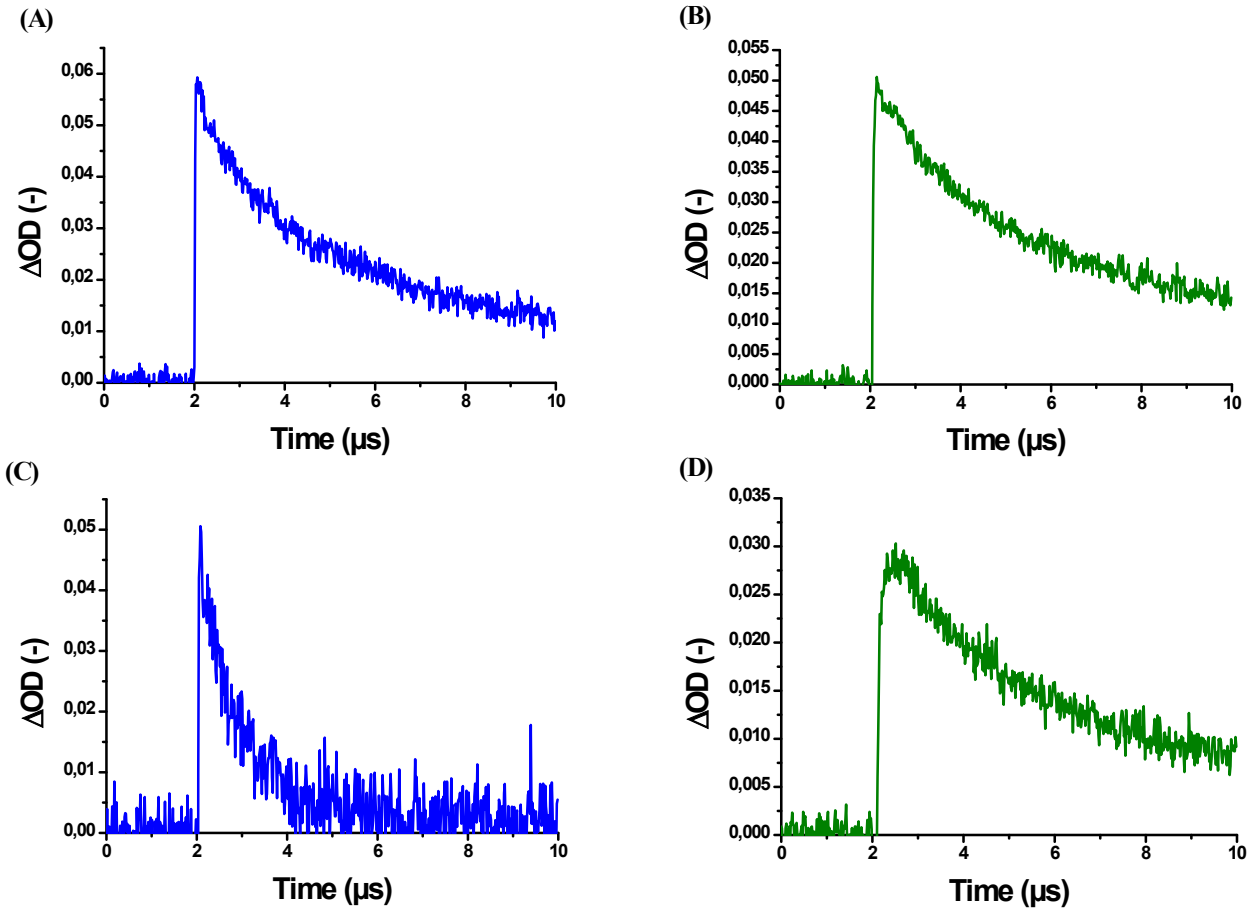

Figure S7: Intersystem crossing quantum yield measurement - Decay traces under nitrogen in dichloromethane after laser excitation at 355 nm of (A) benzophenone recorded at 530 nm, (B) benzophenone + 1-methylnaphthalene recorded at 425 nm, (C) TX-2CBZ recorded at 650 nm and (D) TX-2CBZ +1-methylnaphthalene recorded at 425 nm

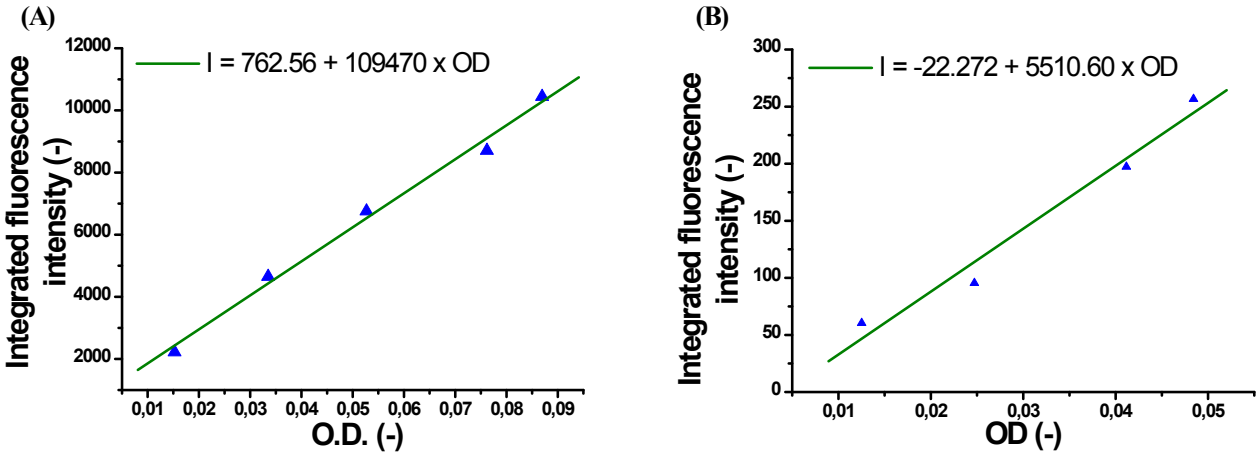

Figure S8: Fluorescence quantum yield measurement – Integrated fluorescence intensity vs absorbance of (A) quinine sulphate in 0.1 M H_2SO_4 and (B) TX-2CBZ in DCM; fluorescence peak integrated from 431 to 639 nm, λ_{ex}=410 nm

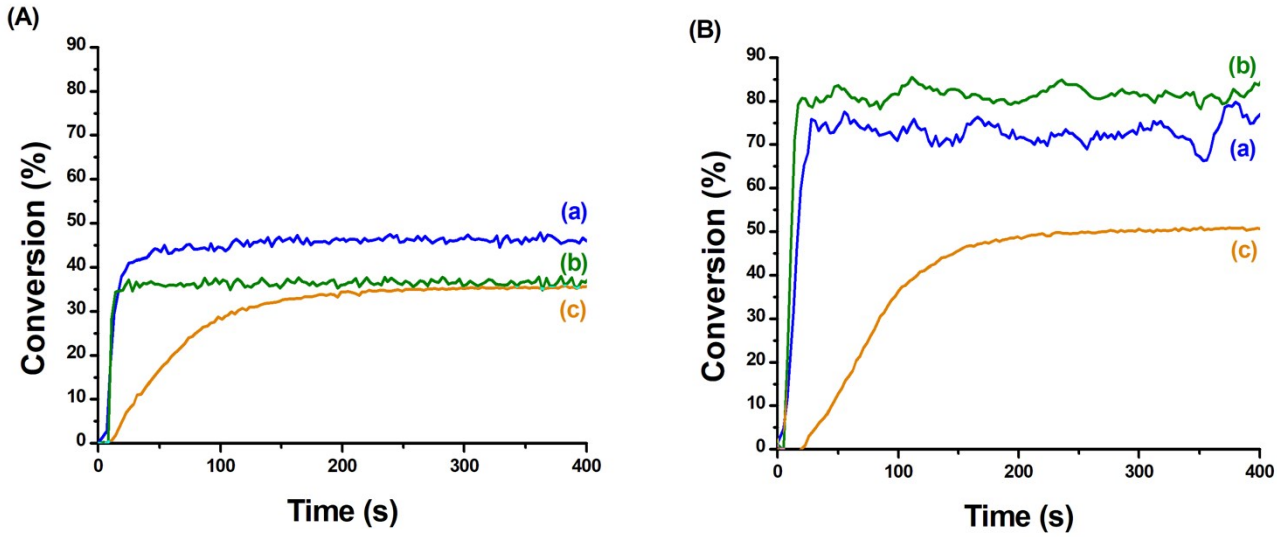

Figure S9: Polymerisation profiles (acrylate function conversion vs irradiation time) of TMPTA upon irradiation with a LED at 405 nm, irradiation starts at 10 s, 50 mW.cm^{-2}; (A) sample thickness = 25 µm and (B) sample thickness = 1.4 mm. Photoinitiating systems: (curve a) TX-2CBZ/Iod (0.07/1.9 w/wt%), (curve b) TX-2CBZ/EDB (0.07/1.9 w/wt%) and (curve c) TX-2CBZ (0.07 w/wt%)

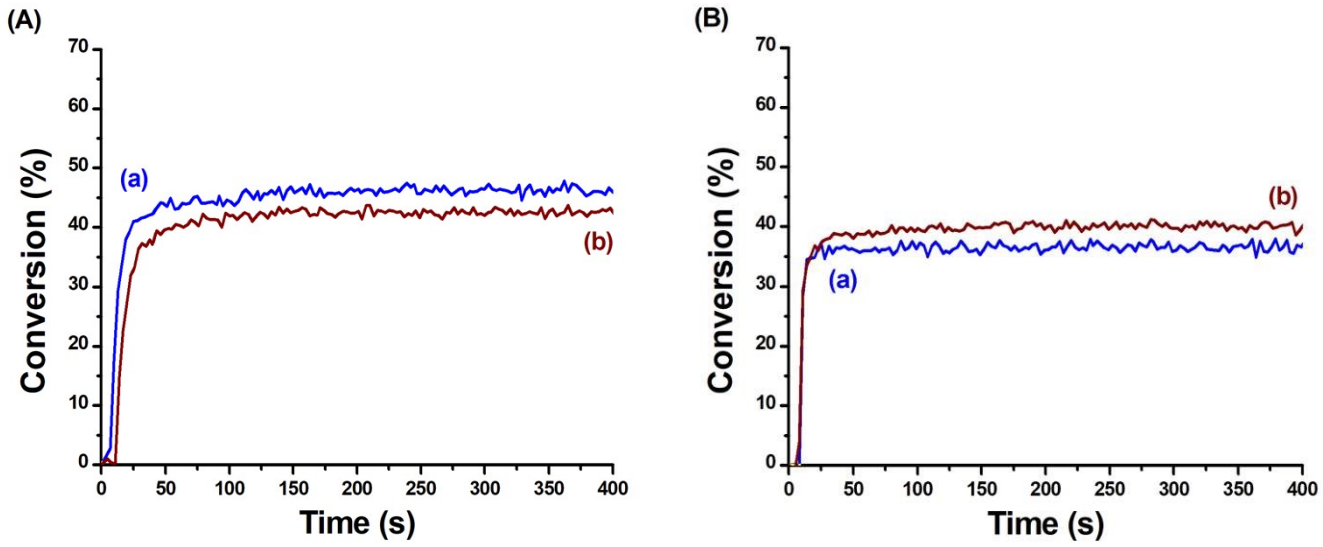

Figure S10: Polymerisation profiles (acrylate function conversion vs irradiation time) of TMPTA upon irradiation with a LED at 405 nm, irradiation starts at 10 s, 50 mW.cm^{-2}; sample thickness = 1.4 mm. (A) Photoinitiating systems: (curve a) TX-2CBZ/Iod (0.07/1.9 w/wt%) and (curve b) ITX/Iod (0.03/2.0 w/wt%), (B) Photoinitiating systems: (curve a) TX-2CBZ/EDB (0.07/1.9 w/wt%) and (curve b) ITX/EDB (0.03/2.0 w/wt%)

Detailed calculation for the assessment of the fluorescence quantum yield, the internal conversion quantum yield, the quantum yield of quenching, and the intersystem crossing quantum yield: example of the system TX-2CBZ in presence of Iod

As stated in the article, the fluorescence quantum yield Φ_f and the intersystem crossing quantum yield Φ_{ISC} have been measured for TX-2CBZ.

$\Phi_f = 0.03$

$\Phi_{ISC} = 0.60 \pm 0.03$

Thus, according to Equation 4:

$\Phi_{IC} = 1 - \Phi_{ISC} - \Phi_f = 1 - 0.60 - 0.03 = 0.37$

In presence of the additive Iod, the quenching reaction should be considered. The singlet quenching quantum yield $\Phi_{q,[IOD]}$ is calculated through Equation 5:

$$\Phi_{q,[Iod]} = \frac{k_q \tau_0 [Iod]}{1 + k_q \tau_0 [Iod]}$$

where $k_q = 6.5 \times 10^9\ L.mol^{-1}.s^{-1}$; $\tau_0 = 7 \times 10^{-9}\ s$; $[Iod] = 0.04\ mol.L^{-1}$

$$\Phi_{q,[Iod]} = \frac{6.5 \times 10^9 \times 7 \times 10^{-9} \times 0.04}{1 + 6.5 \times 10^9 \times 7 \times 10^{-9} \times 0.04} = 0{,}65$$

The fluorescence quantum yield, the internal conversion quantum yield and the intersystem crossing quantum are recalculated for TX-2CBZ in presence of Iod through Equation 6.

$$\Phi_{f,[Iod]} = \frac{\Phi_f}{1 + k_q \tau_0 [Iod]} = \frac{0{,}03}{1 + 6.5 \times 10^9 \times 7 \times 10^{-9} \times 0.04} = 0{,}01$$

$$\Phi_{ISC,[Iod]} = \frac{\Phi_{ISC}}{1 + k_q \tau_0 [Iod]} = \frac{0{,}60}{1 + 6.5 \times 10^9 \times 7 \times 10^{-9} \times 0.04} = 0{,}21$$

$$\Phi_{IC,[Iod]} = \frac{\Phi_{IC}}{1 + k_q \tau_0 [Iod]} = \frac{0{,}37}{1 + 6.5 \times 10^9 \times 7 \times 10^{-9} \times 0.04} = 0{,}13$$

References:

1 L. Ding, Q. Zou, Y. Qu and J. Su, RSC Adv., 2012, 2, 4754–4758.